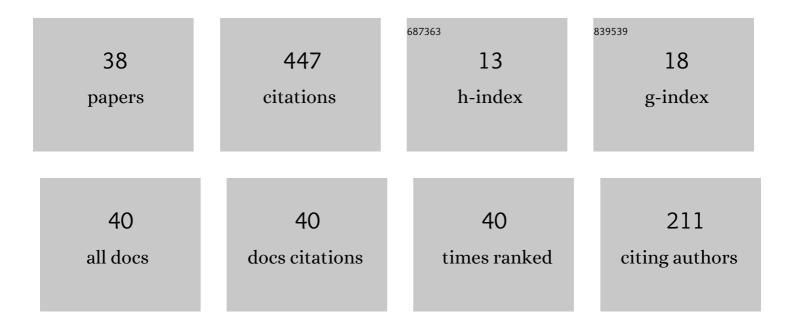
## Kexin Jiao

List of Publications by Year in descending order

Source: https://exaly.com/author-pdf/8835269/publications.pdf Version: 2024-02-01



KEVINILIAO

#	Article	IF	CITATIONS
1	Relationship between interaction under non-load condition and softening & melting behaviour of typical blast furnace feed. Ironmaking and Steelmaking, 2022, 49, 626-633.	2.1	4
2	Comparative Analysis on the Corrosion Resistance to Molten Iron of Four Kinds of Carbon Bricks Used in Blast Furnace Hearth. Metals, 2022, 12, 871.	2.3	5
3	Migration Behavior of K, Na, S, Ti in Hearth of a Commercial Blast Furnace. ISIJ International, 2022, 62, 2236-2243.	1.4	1
4	Melting Erosion Failure Mechanism of Tuyere in Blast Furnace. ISIJ International, 2021, 61, 71-78.	1.4	5
5	Model and application of hearth activity in a commercial blast furnace. Ironmaking and Steelmaking, 2021, 48, 742-748.	2.1	2
6	Investigation of Formation and Shedding Behavior of Slag Crust in a Large Blast Furnace with Copper Stave: Flow Properties and Crystallization Characteristics. Journal of Sustainable Metallurgy, 2021, 7, 506-518.	2.3	7
7	Occurrence State and Behavior of Carbon Brick Brittle in a Large Dissected Blast Furnace Hearth. Steel Research International, 2021, 92, 2100273.	1.8	8
8	Graphitization and Performance of Deadman Coke in a Large Dissected Blast Furnace. ACS Omega, 2021, 6, 25430-25439.	3.5	9
9	Characterization of Ti(C,N) Superstructure Derived from Hot Metal. ISIJ International, 2021, 61, 138-145.	1.4	7
10	Erosion of Carbon Brick by Zinc in Hearth of Blast Furnace. ISIJ International, 2020, 60, 226-232.	1.4	17
11	The influence of basicity and TiO <sub>2</sub> on the crystallization behavior of high Ti-bearing slags. CrystEngComm, 2020, 22, 361-370.	2.6	21
12	A Prediction Model of Blast Furnace Slag Viscosity Based on Principal Component Analysis and K-Nearest Neighbor Regression. Jom, 2020, 72, 3908-3916.	1.9	20
13	Phase Composition and Formation Mechanism of Slag Crust in Blast Furnace. ISIJ International, 2020, 60, 2357-2365.	1.4	6
14	Phase Composition and Properties Distribution of Residual Iron in a Dissected Blast Furnace Hearth. ISIJ International, 2020, 60, 1655-1661.	1.4	4
15	Observation of Deadman Samples in a Dissected Blast Furnace Hearth. ISIJ International, 2019, 59, 1991-1996.	1.4	14
16	Distribution of harmful elements in dissected 125â€m <sup>3</sup> blast furnace. Canadian Metallurgical Quarterly, 2019, 58, 400-409.	1.2	11
17	Thermodynamic Modelling of Iron Ore Sintering Reactions. Minerals (Basel, Switzerland), 2019, 9, 361.	2.0	14
18	Study on Carbothermal Reduction of Titania in Molten Iron. High Temperature Materials and Processes, 2019, 38, 143-150.	1.4	3

Kexin Jiao

#	Article	IF	CITATIONS
19	Insights into Accumulation Behavior of Harmful Elements in Cohesive Zone with Reference to Its Influence on Coke. ISIJ International, 2019, 59, 1796-1800.	1.4	7
20	Temperature Field Distribution of a Dissected Blast Furnace. ISIJ International, 2019, 59, 1027-1032.	1.4	10
21	Status, technological progress, and development directions of the ironmaking industry in China. Ironmaking and Steelmaking, 2019, 46, 937-941.	2.1	14
22	Formation of Multiple Microstructures During the Reduction of Ironsand. Jom, 2019, 71, 1776-1784.	1.9	5
23	Effect of MgO/Al <sub>2</sub> O <sub>3</sub> Ratio on Viscosity of Blast Furnace Primary Slag. High Temperature Materials and Processes, 2019, 38, 354-361.	1.4	13
24	Review of viscosity prediction models of liquid pure metals and alloys. Philosophical Magazine, 2019, 99, 853-868.	1.6	18
25	Damage mechanism of blast furnace tuyere by zinc. Ironmaking and Steelmaking, 2018, 45, 560-565.	2.1	11
26	Melting Features and Viscosity of TiO <sub>2</sub> -Containing Primary Slag in a Blast Furnace. High Temperature Materials and Processes, 2018, 37, 149-156.	1.4	8
27	Effects of Preâ€Reduction Degree of Ironsand on Slag Properties in Melting Separation Process. Steel Research International, 2018, 89, 1700363.	1.8	10
28	Phase Transformation of Cohesive Zone in a Water-quenched Blast Furnace. ISIJ International, 2018, 58, 1775-1780.	1.4	14
29	Graphitization Behavior of Coke in the Cohesive Zone. Metallurgical and Materials Transactions B: Process Metallurgy and Materials Processing Science, 2018, 49, 2956-2962.	2.1	17
30	Viscosity measurement and prediction model of molten iron. Ironmaking and Steelmaking, 2018, 45, 773-777.	2.1	30
31	Behavior of Alkali Accumulation of Coke in the Cohesive Zone. Energy & amp; Fuels, 2018, 32, 8383-8391.	5.1	14
32	Effect of Chlorine on the Viscosities and Structures of CaO-SiO2-CaCl2 Slags. Metallurgical and Materials Transactions B: Process Metallurgy and Materials Processing Science, 2017, 48, 328-334.	2.1	18
33	Analysis on the stamping coke dissolution of hot metal in the blast furnace hearth. Canadian Metallurgical Quarterly, 2017, 56, 205-211.	1.2	5
34	Analysis of the Relationship between Productivity and Hearth Wall Temperature of a Commercial Blast Furnace and Model Prediction. Steel Research International, 2017, 88, 1600475.	1.8	24
35	Gasification Characteristics and Kinetics of Coke with Chlorine Addition. Metallurgical and Materials Transactions B: Process Metallurgy and Materials Processing Science, 2017, 48, 2428-2439.	2.1	6
36	Gaseous Reduction of Titania-ferrous Solution Ore by H <sub>2</sub> –Ar Mixture. ISIJ International, 2017, 57, 443-452.	1.4	9

#	Article	IF	CITATIONS
37	Devolatilization Characteristics and Kinetic Analysis of Lump Coal from China COREX3000 Under High Temperature. Metallurgical and Materials Transactions B: Process Metallurgy and Materials Processing Science, 2016, 47, 2535-2548.	2.1	26
38	Interfaces Between Coke, Slag, and Metal in the Tuyere Level of a Blast Furnace. Metallurgical and Materials Transactions B: Process Metallurgy and Materials Processing Science, 2015, 46, 1104-1111.	2.1	30